after a pulse perturbation does not return to the limit cycle but approaches the steady state. This occurs for low values of φ, which is again in qualitative agreement with experimental results.

The region of attraction of the steady state is in Figure 6 shown in the plane φ versus log K for the amplitude of perturbations $A = 1 \times 10^{-5}$ M. Transitions from the limit cycle to the steady state occur for values of $K = 8 \times 10^{-4}$ to 0.3 s^{-1}. The modeling results are in good agreement with experiments for $K > 3.8 \times 10^{-3}$ s^{-1}. No stopping of oscillations was observed in experiments when $\varphi = 0.5$ to 1.

Conclusions

It was observed in experiments and modeled by a kinetic model that a proper perturbation, applied to one of the two coupled reaction cells that oscillate synchronously, can stop the oscillations and an asymmetric steady state (dissipative structure) sets in. Permanent stopping of oscillations at intermediate values of intensity of mass coupling and transient stopping at low values of the intensity of coupling may serve as a simple example of chemical memory. Similar experimental observations were reported earlier[4] in two coupled cells, and more complicated examples of stationary dissipative systems were discussed in ref 21. Also Crowley and Epstein[22] observed "phase entrainment" and cessation of oscillations in two coupled cells (without perturbation) and used the Oregonator model to interpret the observations.

Registry No. BrO_3^-, 15541-45-4; Ce, 7440-45-1; Br^-, 24959-67-9; malonic acid, 141-82-2.

(21) Stuchl, I.; Marek, M. *J. Chem. Phys.* **1982**, *77*, 2956.
(22) Crowley, M. F.; Epstein, I. R. *J. Phys. Chem.*, in press.

Study of the Recombination Reaction $CH_3 + CH_3 \rightarrow C_2H_6$. 1. Experiment

Irene R. Slagle, David Gutman,*

Department of Chemistry, Illinois Institute of Technology, Chicago, Illinois 60616

Joanne W. Davies, and Michael J. Pilling*

Physical Chemistry Laboratory, South Parks Road, Oxford OX1 3QZ, United Kingdom
(Received: August 11, 1987; In Final Form: November 11, 1987)

The recombination of methyl radicals has been studied as a function of temperature and bath gas density to obtain more detailed knowledge of the kinetics of this reaction in the unimolecular falloff region. The reaction was studied by two techniques: (1) use of a tubular reactor coupled to a photoionization mass spectrometer; (2) use of absorption spectroscopy with a stainless steel flow cell. In both cases, methyl radicals were generated homogeneously by the pulsed photolysis of acetone at 193 nm. CH_3 decay profiles were monitored in real-time experiments. Absolute CH_3 concentrations were obtained from direct measurements of acetone photodecomposition in the photoionization experiments and from previously determined cross sections in the absorption experiments. Rate constants for the $CH_3 + CH_3$ reaction are reported, with argon as the bath gas, at nine temperatures in the range 296–906 K and at gas densities from 1.8×10^{16} to 1.4×10^{19} molecules cm^{-3}. A significantly narrower range of conditions was used in additional experiments using helium as the bath gas. The results obtained are compared with theoretical values of the $CH_3 + CH_3$ recombination rate constant obtained in part 2 (following paper in this issue). The combined results of the experimental and theoretical study of this reaction provide a more quantitative description of the role of collisions in this important recombination process. The uncertainty associated with extrapolating unimolecular rate constants to higher temperatures by using a common functional representation of the pressure and temperature dependence of such rate constants is illustrated with a comparison of theory and extrapolation up to 2000 K for the $CH_3 + CH_3$ high-pressure-limit rate constant.

Introduction

The recombination of methyl radicals (reaction 1) has been and

$$CH_3 + CH_3 + (M) \rightarrow C_2H_6 + (M) \qquad (1)$$

continues to be a reaction of considerable interest to both experimentalists and theoreticians in the field of chemical kinetics. This elementary reaction has been the subject of numerous laboratory studies[1-3] because of its importance as a major termination process in the pyrolysis and oxidation of hydrocarbons,[4,5] its frequent use as a reference reaction in kinetic studies of radical–molecule reactions,[6,7] and its popularity as a model for testing and improving statistical theories of unimolecular reactions.[8-13]

Nearly all the experimental studies of reaction 1 to date have been conducted at or near the high-pressure limit.[1,2] Knowledge of the falloff behavior of this reaction is derived largely from that of the reverse reaction,[1,2,4] the thermal decomposition of ethane.

There have been two experimental studies of reaction 1 in the falloff region. Both have used argon as the collision partner. Glanzer, Quack, and Troe (GQT) measured the apparent bimolecular rate constant k_1 at temperatures close to 1350 K and pressures from 2 to 20 atm.[14] At this temperature, even at 20 atm, reaction 1 was not at the high-pressure limit. More recently,

(1) Baulch, D. L.; Duxbury, J. *Combust. Flame* **1980**, *37*, 313.
(2) Skinner, G. B.; Rogers, D.; Patel, K. B. *Int. J. Chem. Kinet.* **1981**, *13*, 481.
(3) Macpherson, M. T.; Pilling, M. J.; Smith, M. J. C. *J. Phys. Chem.* **1985**, *89*, 2268.
(4) Warnatz, J. In *Combustion Chemistry*; Gardiner, W. C., Ed.; Springer-Verlag: New York, 1984; Chapter 5.
(5) Westbrook, C. K.; Dryer, F. L. *Prog. Energy Combust. Sci.* **1984**, *10*, 1.
(6) Kerr, J. A. In *Free Radicals*; Kochi, J. K., Ed.; Wiley-Interscience: New York, 1973; Vol. 1, Chapter 1.
(7) Kerr, J. A.; Moss, S. J. *CRC Handbook of Bimolecular and Termolecular Gas Reactions*; CRC Press: Boca Raton, FL, 1981.
(8) Waage, E. V.; Rabinovitch, B. S. *Int. J. Chem. Kinet.* **1971**, *3*, 105.
(9) Quack, M.; Troe, J. *Ber. Bunsen-Ges. Phys. Chem.* **1974**, *78*, 240.
(10) Glanzer, K.; Quack, M.; Troe, J. *Chem. Phys. Lett.* **1976**, *39*, 304.
(11) Hase, W. L. *J. Chem. Phys.* **1976**, *64*, 2442.
(12) Wardlaw, D. M.; Marcus, R. A. *J. Phys. Chem.* **1986**, *90*, 5383.
(13) Wardlaw, D. M.; Marcus, R. A. *J. Chem. Phys.* **1985**, *83*, 3462.
(14) Glanzer, K.; Quack, M.; Troe, J. *Symp. (Int.) Combust., [Proc.]* **1976**, *16th*, 949.

0022-3654/88/2092-2455$01.50/0

Macpherson, Pilling, and Smith (MPS) studied reaction 1 as a function both of temperature (296–577 K) and of pressure (5–500 Torr).[3,15] Falloff in k_1 was clearly observed particularly at the higher temperatures (above 400 K) and the lower pressures (below 50 Torr) of this investigation. The rate constants obtained at each temperature were extrapolated to the high- and low-pressure limits by using the method described by Troe[16] to obtain as complete a picture as possible of the high-pressure limit and the falloff behavior of this important recombination reaction.

Recently Hippler, Luther, Ravishankara, and Troe (HLRT) have measured k_1 at ambient temperature in argon from 1 to 200 atm total pressure, thus extending knowledge of the rate constant for reaction 1 to still higher pressures, essentially to the high-pressure limit at this temperature.[17]

To investigate further the role of collisions in the recombination of methyl radicals, we have measured k_1 using photoionization mass spectrometry over a wide temperature range (296–906 K) and at lower pressures (1–10 Torr) than were used in the MPS study discussed above. In addition, the temperature range of the higher pressure experiments of MPS has been extended to 906 K, by using their experimental technique. Argon was again used as the bath gas, and temperatures were chosen to be the same using the two experimental methods. This overlap of conditions was planned to develop an extended view of the falloff behavior of reaction 1 for a particular bath gas over a wide pressure range. In the current investigation, a smaller number of additional measurements of k_1 was also made at three temperatures using helium as the bath gas to provide some knowledge of the effectiveness of a different collision partner in reaction 1.

In part 2 (following paper in this issue),[18] Wagner and Wardlaw present a theoretical study of reaction 1. Values of k_1 are calculated from variational RRKM theory where transition states are identified with the flexible transition-state model developed by Wardlaw and Marcus.[12,13] Two adjustable parameters in the theoretical model are determined from comparisons of values of k_1 obtained by using the theory with those obtained from experiments.

The results of this new experimental investigation of reaction 1 are reported here and presented together with a comparison of the measured values of k_1 with the theoretical values obtained in part 2.

Experimental Section

A. Photoionization Mass Spectrometry. The experimental apparatus used in this study has been described previously.[19] Only a summary is presented here. Pulsed 193-nm radiation from a Lambda Physik EMG 101E excimer laser was directed along the axis of a heatable 1.05-cm i.d. uncoated tubular quartz reactor. Gas flowing through the tube at 4 m s^{-1} contained acetone (the CH_3 source) in low concentration (<1.0%) and the bath gas, argon or helium (>99%). Gas was sampled through a 0.020- or 0.043-cm-diameter tapered hole in the wall of the reactor and formed into a beam by a conical skimmer before it entered the vacuum chamber containing the photoionization mass spectrometer. As the gas beam traversed the ion source, a portion was photoionized and then mass selected. Temporal ion signal profiles were recorded from a short time before each laser pulse to 10–25 ms following the pulse by using a multichannel scalar. Typically data from 1000–5000 experiments were accumulated before the data were analyzed.

Methyl radicals were generated by acetone photolysis (see section C):

$$CH_3COCH_3 \xrightarrow{193\ nm} 2CH_3 + CO \qquad (2)$$

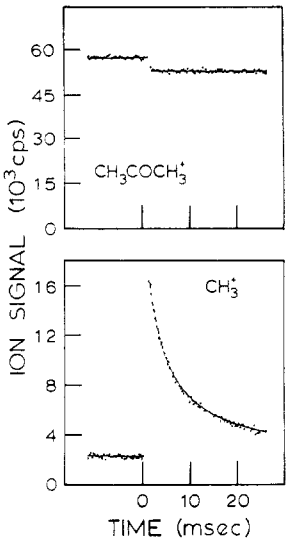

Figure 1. Plot of ion signal profiles recorded during study of reaction 1. Experiments conducted at 810 K. [He] = 2.1×10^{17} atoms cm^{-3}; $[CH_3]_0 = 1.04 \times 10^{13}$ molecules cm^{-3}; $[CH_3COCH_3]_0 = 7.16 \times 10^{13}$ molecules cm^{-3}; acetone decomposition 7.2%. The line through CH_3^+ ion signal profile is the least-squares fit to eq I. The line through $CH_3COCH_3^+$ after $t = 0$ is a straight horizontal line from an average of the data. Measured acetone depletion was used to obtain $[CH_3]_0$.

Instantaneous production of CH_3 by the photolysis of acetone was followed primarily by recombination and, to a minor degree, also by heterogeneous loss:

$$CH_3 + CH_3 + (M) \rightarrow C_2H_6 + (M) \qquad (1)$$

$$CH_3 \rightarrow \text{heterogeneous loss} \qquad (3)$$

The initial CH_3 concentration ($[CH_3]_0$) was determined by measuring the extent of acetone photodecomposition, and the rate constant for reaction 1 was obtained from these concentration measurements and from fits of the measured CH_3^+ temporal ion signal profiles to an analytical expression (given in eq I and II) for $[CH_3]_t$ that is derived from the above mechanism. Sample CH_3^+ and $CH_3COCH_3^+$ ion signal profiles are shown in Figure 1.

The upper density limit at each temperature was fixed by the maximum gas flux that could be tolerated from the gas sampling orifice into the mass spectrometer vacuum chamber. The density range was extended to its present upper limit with the use of a second reactor with a smaller sampling orifice (0.020-cm diameter) for those experiments conducted at the highest three densities.

To control the extent of heating of the system caused by both the relaxation of the acetone photolysis products and by the energy released by the recombination process, we always studied reaction 1 using a large excess of the bath gas over the initial methyl radical concentration ($[CH_3]_0/[Ar] < 1.4 \times 10^{-3}$). The lowest density used at each temperature was determined largely by the desire to keep the temperature rise below 20 K. In most experiments, it was under 10 K.

To obtain some additional knowledge of the kinetics of reaction 1 in a different bath gas, we also conducted a limited number of experiments using helium in large excess.

Source of Gases and Their Purification. Acetone was obtained from Mallinckrodt (99.5% min), and argon (99.996% min) and helium (99.995% min) were obtained from Linde. Acetone was degassed by using freeze–pump–thaw cycles. Argon and helium were used as provided.

Photoionization Energy. Both CH_3 and acetone were detected with the photoionization mass spectrometer using an ionizing energy of 10.2 eV (provided by an H atom resonance lamp).

Determination of k_1. The temporal behavior of $S(CH_3^+)_t$, the CH_3^+ ion signal (which is proportional to $[CH_3]_t$), is given in eq I. This equation takes into account loss of CH_3 by both reactions

$$S(CH_3^+)_t = S(CH_3^+)_0 k_3 \exp(-k_3 t)/[2k_1'(1 - \exp(-k_3 t)) + k_3] \quad (I)$$

(15) Macpherson, M. T.; Pilling, M. J.; Smith, M. J. C. *Chem. Phys. Lett.* **1983**, *94*, 430.
(16) Troe, J. *Ber. Bunsen-Ges. Phys. Chem.* **1983**, *87*, 161.
(17) Hippler, H.; Luther, K.; Ravishankara, A. R.; Troe, J. *Z. Phys. Chem. Neue Folge* **1984**, *142*, 1.
(18) Wagner, A. F.; Wardlaw, D. M., following paper in this issue.
(19) Slagle, I. R.; Gutman, D. *J. Am. Chem. Soc.* **1985**, *107*, 5342.

TABLE I: Conditions and Results of Experiments Using Photoionization Mass Spectrometry To Measure Rate Constants for Methyl Radical Recombination

T^a/K	10^{-16}[M]/ (molecules cm^{-3})	$10^{-13}[CH_3COCH_3]_0$/ (molecules cm^{-3})	$10^{-12}[CH_3]_0$/ (molecules cm^{-3})	k_3/s^{-1}	$10^{11}k_1$/ (cm^3 molecule^{-1} s^{-1})
			M = Ar		
296	3.78	4.24–16.5	2.11–10.9	6.0–8.8	4.4
	7.90	6.03–17.3	3.82–11.4	6.0	4.8
	16.7	2.37–7.31	2.39–6.65	4.4	4.5
	17.3	4.41–11.5	2.51–7.46	4.0	4.4
	34.1	5.61–14.0	2.45–6.64	4.0	5.2
474	1.88	4.58–16.0	4.46–25.4	0.0–2.1	1.9
	3.79	4.94–16.8	5.80–20.2	0.0–2.1	2.2
	7.78	4.94–16.7	5.37–18.6	7.0	2.8
	16.9	3.32–11.0	3.30–14.3	0.4	3.4
	30.9	3.00–13.6	3.00–16.7	0.0	3.8
577	1.94	5.97–17.8	6.70–17.8	0.4–0.5	1.2
	3.65	7.46–22.2	6.86–21.4	3.4	1.4
	7.90	4.95–15.0	7.25–22.2	0.0	1.9
	16.9	3.57–16.8	4.05–18.7	10.3–10.6	2.2
	29.6	3.89–25.3	3.91–23.0	8.4	2.7
700	1.85	6.07–17.0	7.36–17.3	1.6–2.6	0.70
	3.94	11.5–48.3	17.4–50.3	1.6–3.7	0.84
	7.92	2.46–7.46	3.36–10.2	0.0	1.3
	16.9	4.38–13.5	5.60–14.3	0.2	1.8
	28.0	5.39–17.8	6.01–21.5	0.2	2.1
810	1.93	7.41–23.0	6.24–19.9	0.0–2.8	0.43
	3.94	11.7–47.8	16.6–53.6	0.0–2.8	0.51
	7.92	7.45–24.4	8.70–27.3	0.0	0.89
	16.9	6.10–20.0	6.76–26.3	5.6	1.1
	26.4	6.12–20.3	7.30–26.0	5.6	1.2
906	3.98	8.56–40.8	7.19–46.0	0.9–4.0	0.34
	7.93	24.6–69.7	18.9–26.9	6.7	0.44
	17.1	19.3–64.4	23.8–74.8	6.0	0.61
			M = He		
296	7.87	2.16–6.20	1.94–6.50	8.5	3.6
	16.8	3.07–9.58	2.88–8.70	7.6	3.7
	34.3	3.30–10.4	3.41–9.77	6.6	3.7
577	7.91	5.06–14.4	5.93–17.1	9.0	1.8
	17.5	3.18–9.72	4.48–14.0	7.0	2.8
	30.7	2.98–8.87	3.66–11.0	6.0	3.0
810	7.94	10.7–34.2	14.7–48.2	8.0	0.83
	16.9	11.4–38.7	13.3–43.8	8.0	1.1
	26.9	7.16–21.7	10.4–30.9	9.0	1.2

[a] Temperature uncertainty: ±3 K (296 K), ±4 K (474 K), ±5 (577 K), ±6 K (>600 K).

1 and 3. Two parameters in eq I, $S(CH_3^+)_0$, which is the ion signal scaling constant, and k_1' (which is $k_1[CH_3]_0$, the CH_3 decay constant) were obtained from a nonlinear least-squares fit of the CH_3^+ ion signal decay profile to eq I. In those experiments in which $k_3 = 0$, eq II was used instead. The value of k_1 was obtained

$$S(CH_3^+)_t = S(CH_3^+)_0/(1 + 2k_1't) \qquad \text{(II)}$$

from k_1' and the measured value of $[CH_3]_0$, which was determined from the observed acetone depletion.

The heterogeneous loss rate constant, k_3, was measured at each temperature and pressure by using a much lower concentration of CH_3 ($< 5 \times 10^{10}$ molecule cm^{-3}). The value obtained was used in eq I in the determination of k_1. Under most experimental conditions above ambient temperature, reaction 3 consumed a very minor fraction of the methyl radicals. The small effect of reaction 3 on the overall loss of CH_3 is apparent when the data from an experiment are reanalyzed by ignoring the heterogeneous loss of CH_3, i.e., analyzed by using eq II. In those experiments in which $k_3 > 0$, the recalculated values of k_1 are from 1% to 10% higher (2% was typical) than the correct values, i.e., those obtained by using eq I.

The accuracy of the data analysis and gas handling procedures was repeatedly tested. At least two experiments were performed under each set of experimental conditions (T, [M]) by using initial CH_3 concentrations that were at least a factor of 3 apart (to as much as a factor of 8 apart). $[CH_3]_0$ was changed by altering either the laser fluence or the acetone concentration. The measured values of k_1 at each T and [M] were generally less than 10% from the mean value even when the CH_3 half-life varied by 800% in such a group of experiments. This kind of precision was obtained under all experimental conditions.

The measured values of k_1 are estimated to have a most probable accuracy of ±20%. This estimate takes into account the probable uncertainties in the measured experimental parameters (T, [M], $[CH_3]_0$, and k_1) and a small possible systematic error to higher values of k_1 (<1% higher) that arises due to fluctuations of the photolysis laser fluence (which are under ±25% standard deviation). Such a systematic error is caused by averaging the CH_3^+ ion signal decay profiles from experiments in which there is a range of initial CH_3 concentrations.[20]

The conditions of all experiments and the results obtained are given in Table I. The data presented in each line of the table are for a group of experiments conducted to determine k_1 at a particular temperature and gas density. The range of conditions ($[CH_3COCH_3]_0$, $[CH_3]_0$, and k_3) in such a group of experiments is presented along with the average of the several determinations of k_1. The heterogeneous loss constant, k_3, varied in such a set of experiments only if more than 1 day was required to complete the study at a particular T and [M]. Experiments were conducted with M = Ar at temperatures also employed in the absorption experiments. In addition a limited set of experiments was performed with M = He.

B. Absorption Spectroscopy. Details of these experiments including the apparatus and the methods of data analysis employed in the absorption experiments have been previously described.[3,15,20]

(20) Tulloch, J. M.; Macpherson, M. T.; Morgan, C. A.; Pilling, M. J. *J. Phys. Chem.* **1982**, *86*, 3812.

Some changes have recently been made. The pulsed 193-nm radiation is provided by a Lumonics TE861S-4 excimer laser whose output is defocussed with a 5-cm focal length Spectrosil lens. The homogeneous central section of the beam is directed through a stainless steel cell fitted with Spectrosil windows that are sealed onto water-cooled flanges with O rings. This cell replaces the previous all-Spectrosil system with a design that is capable of being used at the higher temperatures employed in the present study. The cell is heated with cartridge heaters, and the temperature controlled and monitored by using two type K thermocouples that are placed both above and below the reaction zone. The reactant gases were flowed through the cell so that the gas mixture was replenished between laser pulses. Flow rates were controlled and measured by using Brooks Instruments 5835 flow controllers and MKS FM360 flow meters, respectively, which were both regularly calibrated by using bubble flow meters. The cell pressure was measured with an MKS Baratron 1000-Torr capacitance manometer.

The methyl radicals were monitored at right angles to the photolysis beam by using a 2-cm path length defined by rectangular collimators in the cell. Light from a 450-W xenon lamp was passed through the cell and then dispersed by a Hilger Watts 1-m Monospeck monochromator. The radicals were detected at 216.36 nm, with a 0.6-nm band-pass. The signals were digitized, averaged, typically with 512 repetitions of the experiment, and analyzed with a microcomputer using a second-order decay function. The variable parameters were the initial absorbance, Δ_0, and k_1/σ, where σ is the absorption cross section of CH_3. A nonlinear least-squares fitting method was employed.[21] σ has been determined experimentally[3] by two independent techniques at room temperature and by one of these techniques over the temperature range 296–537 K. The temperature dependence of the measured values was compared with that of relative cross sections calculated by Quack[22] and by Ashfold.[23] The agreement was good. The calculated temperature dependence has been employed in the present study to extend the absolute cross sections up to 906 K. Over the lower temperature range (296–577 K), a linear function was used to describe the temperature dependence of σ:

$$10^{17}\sigma/\mathrm{cm}^2 = 5.90 - 5.95 \times 10^{-3}(T/\mathrm{K}) \qquad \text{(III)}$$

At higher temperatures (>700 K), a quadratic dependence is required:

$$10^{17}\sigma/\mathrm{cm}^2 = 7.58 - 1.29 \times 10^{-2}(T/\mathrm{K}) + 7.28 \times 10^{-6}(T/\mathrm{K})^2 \qquad \text{(IV)}$$

The uncertainty in the high-temperature cross section is estimated to be ±10% (two standard deviations).

The validity of the second-order fit was checked for all experimental conditions. The residuals were inspected visually and were found to be randomly scattered about zero. The inclusion of a first-order loss process at high temperatures (vide infra) had a negligible effect on the fitted values of k_1/σ.

The values of k_1 obtained in these experiments (and of σ at each temperature) are presented in Table II together with estimates of their uncertainties. The table includes both the data obtained in the present set of experiments (700–906 K) and those previously reported by MPS (296–577 K). The latter have been included not only for completeness but also because, in their original published form,[15] a still earlier estimate of the absorption cross section was employed. A complete listing of the revised rate constants was not presented in the paper reporting the new determinations of $\sigma(T)$.[3]

The error estimates in Table II include contributions from σ, from k_1/σ (estimated from the scatter of eight independent experimental determinations of k_1/σ at each temperature and pressure), and from uncertainties in T and P propagated via the dependence of k_1/σ and σ on these two parameters. The shot-to-shot reproducibility of the excimer laser during the accumulation of each decay profile was better than ±5%, so any error introduced into the measurements of k_1/σ from variations in $[CH_3]_0$ was negligible.[20] It is difficult to make an estimate of additional sources of possible systematic errors, so no such contribution is included in the tabulated standard deviations, which must, therefore, be regarded as *lower* limits. In this respect, it should be noted that the latest measurements were made with an entirely redesigned cell with a much shorter path length. Checks at 296 K yielded experimental values of k_1/σ in agreement (within quoted limits) with those determined by MPS with the original apparatus.

Sources of Gases and Their Purification. Acetone was obtained from BDH Chemicals Ltd. (99.8%) and purified by passing it twice through a $CaCl_2$ column followed by repeated freeze–pump–thaw cycles. Argon (BOC Ltd., 99.998%) was used without additional purification.

C. Photolysis System. The photolysis of acetone at 193 nm, which was used in this study as the methyl radical source, has been shown by Lightfoot et al. to proceed predominantly (>96%) via reaction 2 under conditions similar to those used in the current investigation.[21] In this study, two additional single-photon processes were identified, and their importances measured:

$$CH_3COCH_3 \xrightarrow{193\ \mathrm{nm}} H + CH_2COCH_3 \qquad (4)$$

$$CH_3COCH_3 \xrightarrow{193\ \mathrm{nm}} CH_4 + CH_2CO \qquad (5)$$

Reactions 4 and 5 occur to minor degrees: ≤2.5% for reaction 4 and ≤1.5% for process 5. Secondary photolysis of CH_3, which was observed to occur to a minor degree during the photolysis of azomethane, was negligible under the present conditions.

In the analysis of the photoionization experiments, no account was taken of the minor acetone photolysis routes. The value of $[CH_3]_0$ was taken to be twice that of the measured depletion in the acetone concentration. The effect of this small systematic overdetermination of CH_3 on the determination of k_1 is largely offset by disregarding the minor additional recombination process, $CH_3 + CH_2COCH_3$, which consumes methyl radicals and is not taken into account in the data analysis.

The minor routes were also ignored in the analysis of the decay profiles of the absorption experiments (although they were included in the determination of σ, which yielded a correction of only 0.4%).[3] Simulations of the reaction kinetics following azomethane photolysis (where minor routes are slightly more important) demonstrated that the rate of CH_3 decay is increased by <0.5% by the other possible recombination reactions.[3]

The CH_3 radicals are produced with an excess of vibrational and translational energy by the photolysis of acetone at 193 nm.[24,25] The experimental measurements of the vibrational relaxation rate constant of CH_3 in argon and helium by Donaldson and Leone[25] indicate that, under our experimental conditions, the vibrational relaxation time of CH_3 is much shorter than the recombination half-life (by at least a factor of 100). Confirmation of this fact was provided by observations in the absorption experiments, where, at short times and at low pressures (≈1 Torr), absorption by the ground vibrational state of CH_3 was observed to grow on a microsecond time scale while relaxation of the higher states occurred.[15]

At the higher temperatures of this study, the possible effects of two high activation energy processes need to be assessed.

H Atom Abstraction by CH_3. For the reaction

$$CH_3 + CH_3COCH_3 \rightarrow CH_4 + CH_2COCH_3 \qquad (6)$$

Ferguson and Pearson[26] report an Arrhenius expression for $k_6 = 5.3 \times 10^{-13} \exp[-(4850 \pm 95)/T]$ cm^3 molecule^{-1} s^{-1}. This reaction

(21) Lightfoot, P. D.; Kirwan, S. D.; Pilling, M. J., manuscript in preparation.
(22) Quack, M., private communication.
(23) Ashfold, M. N. R., private communication.

(24) Donaldson, D. J.; Leone, S. R. *J. Chem. Phys.* **1986**, *85*, 817.
(25) Donaldson, D. J.; Leone, S. R. *J. Phys. Chem.* **1987**, *91*, 3128.
(26) Ferguson, K. D.; Pearson, J. T. *Trans. Faraday Soc.* **1970**, *66*, 910.

TABLE II: Conditions and Results of Experiments Using Absorption Spectroscopy To Measure Rate Constants for Methyl Radical Recombination (M = Ar)

T/K	P/Torr	10^{-16}[M]/ (molecules cm^{-3})	$10^{11}(k^a \pm 2SD^b)$/ (cm^3 molecule^{-1} s^{-1})	$10^{17}(\sigma^c + 2SD)$/ cm^2	T/K	P/Torr	10^{-16}[M]/ (molecules cm^{-3})	$10^{11}(k^a \pm 2SD^b)$/ (cm^3 molecule^{-1} s^{-1})	$10^{17}(\sigma^c + 2SD)$/ cm^2
296	5.39	17.6	5.14 ± 0.22	4.14 ± 0.15	577	5.12	8.56	1.74 ± 0.14	2.47 ± 0.17
	14.3	46.6	5.32 ± 0.22			6.87	11.5	1.87 ± 0.15	
	41.1	134	5.61 ± 0.21			9.48	15.9	2.04 ± 0.14	
	101	329	5.78 ± 0.21			12.4	20.7	2.32 ± 0.21	
	244	796	5.90 ± 0.22			17.0	28.4	2.59 ± 0.19	
	493	1610	5.92 ± 0.22			24.6	41.2	2.76 ± 0.19	
407	6.05	14.4	4.09 ± 0.20	3.48 ± 0.12		29.4	49.2	2.74 ± 0.22	
	9.61	22.8	4.29 ± 0.19			43.4	72.6	2.96 ± 0.21	
	14.1	33.4	4.29 ± 0.18			65.6	110	3.18 ± 0.23	
	25.6	60.7	4.67 ± 0.20			95.2	159	3.36 ± 0.23	
	51.2	121	4.92 ± 0.18			130	217	3.53 ± 0.25	
	194	460	5.21 ± 0.21			222	371	3.61 ± 0.30	
	411	975	5.08 ± 0.18			394	659	3.77 ± 0.28	
474	7.66	15.6	3.22 ± 0.20	3.08 ± 0.13	700	25.1	34.6	2.09 ± 0.23	2.15 ± 0.22
	7.97	16.2	3.14 ± 0.20			35.6	49.1	2.03 ± 0.22	
	8.96	18.2	3.47 ± 0.16			50.4	69.5	2.19 ± 0.24	
	9.97	20.3	3.29 ± 0.16			75.2	104	2.41 ± 0.26	
	12.0	24.4	3.25 ± 0.22			102	141	2.77 ± 0.29	
	17.4	35.4	3.33 ± 0.15			156	216	3.08 ± 0.33	
	20.3	41.3	3.92 ± 0.17			203	280	3.29 ± 0.36	
	24.0	48.9	3.52 ± 0.15			257	354	3.42 ± 0.38	
	31.6	64.3	3.87 ± 0.17			302	416	3.24 ± 0.34	
	43.9	89.4	3.95 ± 0.17			353	487	3.24 ± 0.33	
	66.6	136	4.02 ± 0.17			395	545	3.45 ± 0.36	
	91.5	186	4.42 ± 0.25			449	619	3.48 ± 0.36	
	92.0	187	4.23 ± 0.18			500	689	3.40 ± 0.36	
	152	310	4.71 ± 0.20			554	764	3.56 ± 0.37	
	390	794	5.17 ± 0.23			591	815	3.52 ± 0.36	
513	11.3	21.3	2.92 ± 0.20	2.85 ± 0.14	810	52.1	62.1	1.65 ± 0.22	1.95 ± 0.19
	18.8	35.4	3.07 ± 0.22			74.4	88.6	1.85 ± 0.24	
	27.7	52.1	3.43 ± 0.19			109	129	1.81 ± 0.22	
	41.0	77.1	3.68 ± 0.22			152	181	2.22 ± 0.26	
	58.0	109	3.65 ± 0.19			201	240	2.36 ± 0.27	
	80.0	151	3.89 ± 0.19			252	300	2.42 ± 0.26	
	126	237	4.00 ± 0.21			300	357	2.58 ± 0.31	
539	7.15	12.8	2.47 ± 0.33	2.69 ± 0.15		349	416	2.68 ± 0.28	
	9.07	16.2	2.53 ± 0.21			402	479	2.65 ± 0.28	
	12.8	22.9	2.80 ± 0.18			453	539	2.99 ± 0.32	
	16.7	29.9	2.84 ± 0.20			501	597	3.06 ± 0.34	
	20.8	37.2	3.12 ± 0.20			549	654	3.10 ± 0.34	
	25.4	45.5	3.10 ± 0.18			598	713	3.04 ± 0.32	
	30.9	55.3	3.15 ± 0.20		906	74.3	79.2	1.48 ± 0.26	1.91 ± 0.19
	41.3	74.0	3.31 ± 0.21			101	107	1.52 ± 0.24	
	62.2	111	3.49 ± 0.23			154	165	1.79 ± 0.26	
	90.7	162	3.74 ± 0.21			201	214	2.04 ± 0.24	
	130	233	4.01 ± 0.23			251	267	2.20 ± 0.25	
	180	322	4.07 ± 0.24			303	322	2.27 ± 0.25	
	273	489	4.10 ± 0.25			351	374	2.19 ± 0.24	
	430	770	4.24 ± 0.24			398	424	2.50 ± 0.27	
						450	480	2.40 ± 0.26	
						501	534	2.57 ± 0.27	
						550	586	2.78 ± 0.32	
						599	638	2.87 ± 0.33	

[a] Rate constants over the temperature range 296–577 K were previously reported in ref 15, where an early estimate of σ was employed. The values given here incorporate the measured σ values reported in ref 3. In addition, the original data have been reanalyzed, leading to slight variations in the values of k/σ. [b] Error limits quoted refer to ±2 standard deviations. The determinations of the standard deviations is discussed in the text. [c] Determination of the absorption cross sections over the range $296 \leq T/K \leq 537$ is described in ref 3. The calculation of σ at higher temperatures is discussed in the text.

was a negligible loss process for CH_3 under the conditions of all experiments. Under the most unfavorable conditions (i.e., at 906 K and for the lowest $[CH_3]_0$ values used), the pseudo-first-order rate constant for removal of CH_3 via reaction 6 was <1% of $2k_1[CH_3]_0$, therefore the effect of this reaction on the decay of CH_3 is negligible. Mixed-order fits to the decay data, in which reaction 6 was included, returned essentially unchanged values for k_1.

CH_3 Production Due to Acetone Decomposition. The thermal decomposition of acetone in the heated reactor provides a negligible contribution to the initial concentration of CH_3 in these experiments. Therefore it was not necessary to take this process into account in determining $[CH_3]_0$. Acetone can decompose thermally via a chain mechanism:

$$CH_3COCH_3 \rightarrow 2CH_3 + CO \quad (7)$$

$$CH_3 + CH_3COCH_3 \rightarrow CH_4 + CH_2COCH_3 \rightarrow CH_2CO + CH_3 \quad (6)$$

After including reaction 1 in the above mechanism, one can calculate the steady-state concentration of CH_3: $[CH_3]_s = (k_7[CH_3COCH_3]/k_1)^{1/2}$. With use of $k_7 = 2.4 \times 10^{14} \exp(-36\,000/T)$ s^{-1},[27] it is possible to calculate $[CH_3]_s/[CH_3]_0$ for all experimental conditions. Again, with use of the most unfavorable case to establish an upper limit for this ratio (906 K and the lowest laser fluences used), this ratio of thermal methyl radicals to those produced photolytically was always below 5×10^{-3}, which is a negligible fraction of the initial CH_3 concentration produced by photolysis. An insignificant fraction of the acetone decomposed during the flow of gases through the reactors.

Discussion

A. Comparisons with Prior Measurements of k_1. The agreement between the experimental measurements of k_1, obtained

(27) Swarc, M.; Watson Taylor, J. J. *J. Chem. Phys.* **1955**, *23*, 2310.

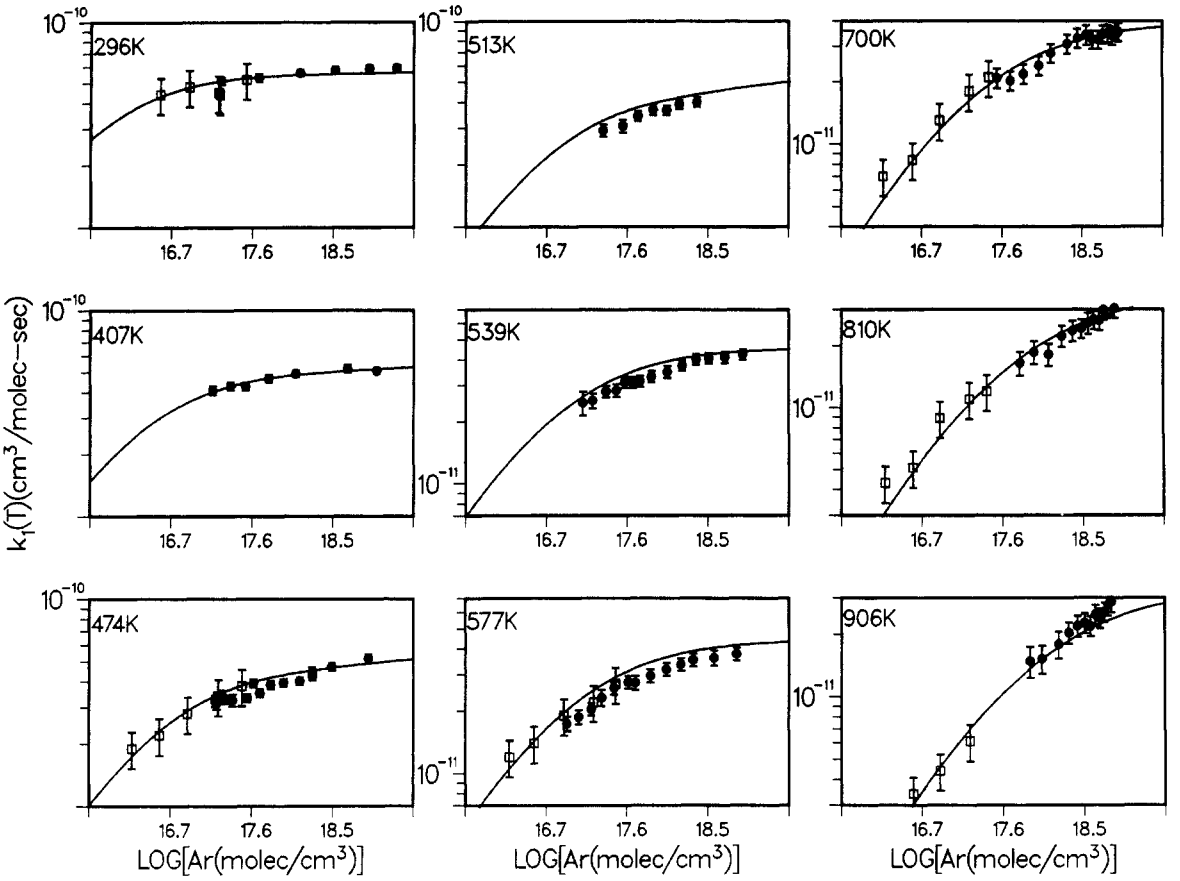

Figure 2. Comparison of measured and calculated values of k_1 versus Ar bath gas density: open squares, photoionization mass spectrometry (see Table I); closed circles, absorption spectroscopy (see Table II). Vertical lines are stated error limits. Continuous lines on plots are calculated values of k_1 from part 2.[18]

by using two different techniques at six common temperatures, is apparent in the plot of the results in Figure 2. At the three lower temperatures ($T \leq 577$ K), where there is an overlap of the pressure ranges used in the two investigations, there is satisfactory agreement, especially at 296 K. At 474 and 577 K, a small systematic disparity between the two sets of data (<10%) is well within the combined uncertainty estimates of both investigations. It is more difficult to assess the level of agreement for $T \geq 700$ K because the pressure ranges of the two parts of this study did not overlap. (With the new absorption cell it was not possible to conduct experiments at pressures as low as were used by MPS, particularly at these elevated temperatures.)

At room temperature, both sets of measurements of k_1 are also in very good agreement (when appropriately extrapolated; see below) with the high-pressure measurements of HLRT,[17] who report $k_1(296\ K, \infty) = (5.8 \pm 0.6) \times 10^{-11}$ cm^3 molecule^{-1} s^{-1}.

B. Comparisons with Theoretical Values of k_1. In part 2, theoretical values of k_1 are presented that were calculated by using variational RRKM theory.[18] Flexible structures along the reaction coordinate are used to identify and characterize transition states.[12,13]

The existence of additional high-temperature channels for the $CH_3 + CH_3$ reaction was not considered in the theoretical model. While these channels are responsible for the *net* loss of CH_3 in the $CH_3 + CH_3$ reaction at temperatures above those at which C_2H_6 is a stable product (i.e., above 1500 K),[28,29] the decomposition of C_2H_6* formed in reaction 1 back to the original reactants is strongly favored under all conditions over the alternate endothermic decomposition channels that form other products (e.g., $C_2H_5 + H$). The high-temperature routes are a small perturbation on the main reversible reaction, the formation of C_2H_6 and its dissociation back to methyl radicals.

Two parameters were varied to obtain optimum agreement between theory and experiment: α (a potential parameter that determines the tightness of the transition states) and $\langle \Delta E \rangle_{tot}$ (the average energy change in collisions between metastable C_2H_6* formed in reaction 1 and the bath gas). The optimum values of these two parameters are 0.70 Å^{-1} for α and −205 cm^{-1} for $\langle \Delta E \rangle_{tot}$ (M = Ar). The internal parameter α was selected to obtain agreement at the high-pressure limit (at ambient temperature), where the rate constant is well-known and is also not sensitive to the role of collisions. Its value was adjusted to obtain a calculated value of k_1 (296 K, ∞) that is the same as the measured value reported by HLRT.[17] A comparable value (within 5%) of k_1 (296 K, ∞) was also obtained directly from the measured rate constants by using a global procedure (see below).

From the small set of experiments in which helium was the bath gas, a value of $\langle \Delta E \rangle_{tot} = -135$ cm^{-1} was indicated (α remains unchanged since its value is chosen to obtain the best agreement between theory and experiment at the high-pressure limit).

Calculated falloff curves for k_1 (for M = Ar) determined in part 2[18] are shown in Figure 2 superimposed on the plot of the measured rate constants. Agreement with the rate constants determined in the current study is very good at all temperatures and densities. The weighted average deviation of the measured values from the theoretical ones is 9.9%. In addition, theoretical values of k_1 at 1350 K are very close to the measured values of k_1 at this temperature reported by GQT[10] (see part 2 for a complete discussion of these comparisons[18]).

The calculated falloff curves for M = He are shown in Figure 3 together with the few measured values obtained in the current investigation. A value of $\langle \Delta E \rangle_{tot}$ chosen to obtain reasonable agreement between theory and experiment at the two elevated temperatures results in substantially less agreement at ambient temperature than is the case when argon is the bath gas. The cause of this poorer agreement is uncertain. More experiments are planned to obtain a clearer picture of the kinetics of reaction 1 with this bath gas.

(28) Roth, P.; Just, T. *Ber. Bunsen-Ges. Phys. Chem.* **1979**, *83*, 577.
(29) Kiefer, J. H.; Butach, K. A. *Int. J. Chem. Kinet.* **1984**, *16*, 679.

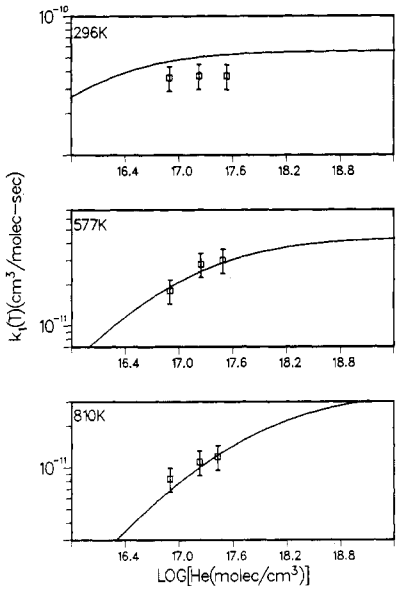

Figure 3. Comparison of measured and calculated values of k_1 versus He bath gas density: open squares, current study (see Table I). Lines on plots are calculated values of k_1 from part 2.[18]

C. Analytical Expression for $k_1(T,M)$. It is advantageous for chemical kinetic modeling purposes to express k_1 as an analytic function of temperature and pressure. Theoretical values of k_1 for M = Ar were fit in part 2[18] to an expression introduced by Troe:[30]

$$\log k_1 = \log [k_0/(1 + k_0/k_\infty)] + \log (F_{cent})/\{1 + [\log (k_0/k_\infty)]^2\} \quad \text{(ref 16)} \quad \text{(V)}$$

The form of the temperature-dependent functions used for k_0 (the low-pressure-limit rate constant times the gas density), k_∞ (the high-pressure-limit rate constant), and F_{cent} (the broadening parameter) are those suggested by Gilbert et al.[31]

$$k_0 = 8.76 \times 10^{-7} T^{-7.03} \exp(-1390/T)[\text{Ar}] \text{ cm}^3 \text{ molecule}^{-1} \text{ s}^{-1} \quad \text{(VI)}$$

$$k_\infty = 1.50 \times 10^{-7} T^{-1.18} \exp(-329/T) \text{ cm}^3 \text{ molecule}^{-1} \text{ s}^{-1} \quad \text{(VII)}$$

$$F_{cent} = 0.381 \exp(-T/73.2) + 0.619 \exp(-T/1180) \quad \text{(VIII)}$$

The numerical parameters in eq VI–VIII were obtained from fits to theoretical values of k_1 calculated over a broad range of conditions: $200 \leq T/\text{K} \leq 2000$ and over a density range at each temperature that corresponded to values of k_1 from 1×10^{-12} molecule^{-1} s^{-1} to the high-pressure limit.

The relative root mean square deviation between the measured rate constants and those obtained by using eq V (with the parameters in eq VI–VIII) is ±11.2%. This deviation is slightly larger than that between the theoretical and measured rate constants. The slight decrease in accuracy in k_1 values resulting from use of eq V is offset by the convenience of having an analytical expression to calculate this rate constant over a wide range of conditions.

Because the parameters in eq VI–VIII are derived from a detailed theoretical model for reaction 1, their use in eq V is expected to yield accurate values of k_1 over a wider range of conditions than were covered by experiment and in particular over the temperature and density ranges used in the fitting procedure. Far less reliable extrapolations are obtained by using only the measured values of $k_1(T,\text{M})$ in Tables I and II without the help of the theoretical model to obtain temperature-dependent expressions for k_0, k_∞, and F_{cent}. For example, the rate constants in Tables I and II were fit to an equation analogous to eq V (eq 1, ref 31) by using a global technique recently developed by Keiffer et al.[32] Five parameters were varied, A_∞, n_∞, A_0, n_0, and $\langle \Delta E \rangle_{down}$, with k_∞ and k_0 given by[33]

$$k_0 = A_0 T^{n_0}[\text{Ar}] \qquad k_\infty = A_\infty T^{n_\infty} \quad \text{(IX)}$$

(More complex functions to express these temperature dependencies are not warranted by the experimental results alone. The temperature dependencies of k_0 and k_∞ (even between 296 and 906 K) are too small to suggest more appropriate functions for $k_0(T)$ and $k_\infty(T)$ without the aid of a theoretical model.) While the global procedure fitted the experimental data just as well as the theoretical model did, it yielded quite different values of k_1 on extrapolation to higher temperatures. For example, the temperature dependence of k_∞ in eq IX is not able to reproduce the strong decrease in k_∞ at higher temperatures that is predicted by the theoretical model (see Figure 4).[18] Calculation of k_1 at 2000 K and 1 atm (with k_0 and k_∞ given by eq IX) yields a value 3 times higher than that obtained by using eq V–VIII at this temperature. Expressions like those in eq IX, which can provide accurate interpolations of the temperature dependencies of k_0 and k_∞ (as well as of the temperature and pressure dependence of k_1), should be used with caution for extrapolations significantly outside the range of conditions used to establish the parameters in these expressions.

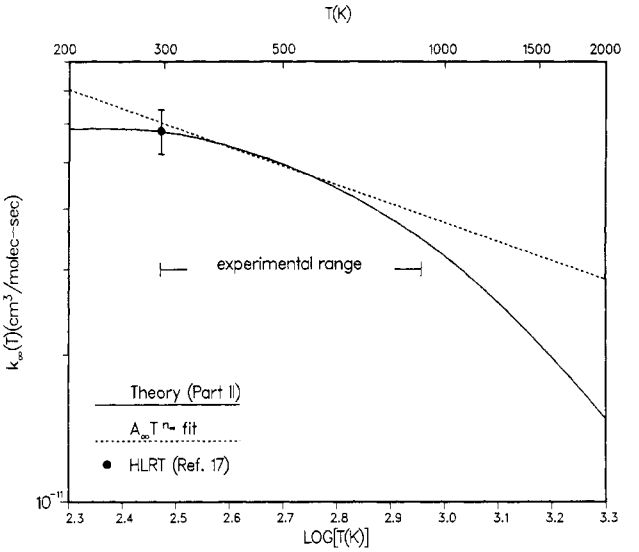

Figure 4. Comparison between the high-pressure-limit rate constants (k_∞) for reaction 1 obtained from the theoretical model and the function $k_\infty = A_\infty T^{n_\infty}$, shown to illustrate the inability of this function to simultaneously account for the temperature dependence of k_∞ in the experimental range $296 \leq T/\text{K} \leq 906$ and the strong decrease in k_∞ at higher temperatures predicted by the theoretical model.

Summary

This combined experimental and theoretical study of reaction 1 (parts 1 and 2) provides a more quantitative and detailed picture of the kinetics of this important recombination reaction over a wide range of experimental conditions. The ability of the theoretical model to yield accurate values of k_1 throughout the falloff region over a considerable temperature range (296–1350 K) demonstrates its accuracy and indicates its usefulness for predictive purposes. A parametrized version of $k_1(T,\text{M})$ determined in part 2 is also included in this report since it is recommended for use in calculating values of $k_1(T,\text{M})$ both inside and outside the range

(30) Troe, J. *J. Phys. Chem.* **1979**, *83*, 114.
(31) Gilbert, R. G.; Luther, K.; Troe, J. *Ber. Bunsen-Ges. Phys. Chem.* **1983**, *87*, 169.
(32) Keiffer, M.; Pilling, M. J.; Smith, M. J. C. *J. Phys. Chem.* **1987**, *91*, 6028.
(33) Baulch, D. L.; Cox, R. A.; Hampson, R. F.; Kerr, J. A.; Troe, J. *J. Phys. Chem. Ref. Data* **1984**, *13*, 1259.

of conditions of the current investigation.

Future experiments are planned with helium and other bath gases to extend the present knowledge of the role of collisions in this important recombination reaction.

Acknowledgment. We gratefully acknowledge useful discussions with Albert F. Wagner, David M. Wardlaw, and William C. Gardiner. We also thank Paul F. Sawyer for developing the computer codes used in the data analysis and Dariusz Sarzynski for his assistance in performing experiments (both at IIT). The research at IIT was supported by the Office of Basic Energy Sciences, Division of Chemical Sciences, U.S. Department of Energy under Contract DE-AC02-78ER-14593 and that at Oxford by S.E.R.C.

Registry No. CH_3, 2229-07-4; acetone, 67-64-1.

Study of the Recombination Reaction $CH_3 + CH_3 \rightarrow C_2H_6$. 2. Theory

Albert F. Wagner*

Chemistry Division, Argonne National Laboratory, Argonne, Illinois 60439

and David M. Wardlaw†

Department of Chemistry, Queen's University, Kingston, Ontario, K7L 3N6 Canada
(Received: August 11, 1987; In Final Form: December 15, 1987)

A microcanonical variational RRKM rate constant calculation, based on the flexible transition-state theory of Wardlaw and Marcus (*Chem. Phys. Lett.* **1984**, *110*, 230) and an adjustable semiempirical potential energy surface, is compared to the measurement of part 1 (preceding paper in this issue) and other experimental studies. The calculations contain two adjustable parameters: a potential parameter α, which influences the tightness of the transition state, and $\langle\Delta E\rangle_{tot}$, the total average energy change in metastable C_2H_6* per collision with the buffer gas. When the parameters are optimized, the resulting calculated rate constants have a 9.9% root mean square error with respect to the measurements in Ar buffer gas. The final parameter values are $\alpha = 0.70 \pm 0.13$ Å^{-1} and $\langle\Delta E\rangle_{tot} = -205 \pm 65$ cm^{-1}. Similar calculations for He buffer gas produce 22.4% error when compared to the less extensive measurements and give an optimized $\langle\Delta E\rangle_{tot}$ value of about -135 cm^{-1}. The rate calculations for Ar buffer gas have been extended to 2000 K and then fit over the full temperature and pressure range to a modification of the functional form of Gilbert et al. (*Ber. Bunsen-Ges. Phys. Chem.* **1983**, *87*, 161). The resulting fitted functions required by that form are $k_0 = 8.76 \times 10^{-7} T^{-7.03} e^{-1390/T}$[Ar] cm^3/(molecule s), $F_{cent} = 0.381e^{-T/73.2} + 0.619e^{-T/1180}$, and $k_\infty = 1.50 \times 10^{-7} T^{-1.18} e^{-329/T}$ cm^3/(molecule s). When used in the Gilbert et al. function, this parametrization produces an excellent representation of the theoretical and experimental rate constants in Ar.

I. Introduction

The recombination of methyl radicals in the presence of buffer gas M (reaction 1) has been and continues to be a reaction of

$$CH_3 + CH_3 + M \rightarrow C_2H_6 + M \qquad (1)$$

considerable interest to both experimentalists and theoreticians in the field of chemical kinetics. This elementary reaction has been the subject of numerous laboratory studies[1-7] because of its importance as a major termination process in the pyrolysis and oxidation of hydrocarbons,[8,9] its frequent use as a reference reaction in kinetic studies of radical–molecule reactions,[10,11] and its popularity as a model for testing and improving statistical theories of unimolecular reactions.[3,12-16]

Most of the experimental studies of reaction 1 to date have been conducted at or near the high-pressure limit.[1,2,4] The best available measurement of this limit is in ref 4, where Hippler, Luther, Ravishankara, and Troe (HLRT) have measured k_1 at ambient temperature in Ar from 1 to 200 atm of total pressure. There have been three experimental studies of reaction 1 in the falloff region. The two earliest studies both used argon as the collision partner. Glanzer, Quack, and Troe[3] (GQT) measured the apparent bimolecular rate constant k_1 at temperatures close to 1350 K and pressures from 2 to 20 atm. More recently, Macpherson, Pilling, and Smith[5,6] (MPS) studied reaction 1 as a function both of temperature (296–577 K) and of pressure (5–500 Torr). In the MPS study, the rate constants obtained at each temperature were fit to a pressure-dependent functional form for recombination rate constants introduced by Troe[17] to obtain as comprehensive a picture as possible of the high-pressure limit and the falloff behavior. At room temperature, this high-pressure limit agrees closely with that directly measured by HLRT.

The most recent study of the falloff behavior is described in the collaborative preceding paper,[7] hereafter designated part 1,

† Natural Science and Engineering Research Council of Canada, University Research Fellow.

(1) Baulch, D. L.; Duxbury, J. *Combust. Flame* **1980**, *37*, 313.
(2) Skinner, G. B.; Rogers, D.; Patel, K. B. *Int. J. Chem. Kinet.* **1981**, *13*, 481.
(3) Glanzer, K.; Quack, M.; Troe, J. *Chem. Phys. Lett.* **1976**, *39*, 304.
(4) Hippler, H.; Luther, K.; Ravishankara, A. R.; Troe, J. *Z. Phys. Chem. Neue Folge* **1984**, *142*, 1.
(5) Macpherson, J. T.; Pilling, J. J.; Smith, M. J. C. *Chem. Phys. Lett.* **1983**, *94*, 430.
(6) Macpherson, J. T.; Pilling, J. J.; Smith, M. J. C. *J. Phys. Chem.* **1985**, *89*, 2268.
(7) Slagle, I. R.; Gutman, D.; Davies, J. W.; Pilling, M. J., preceding paper in this issue.
(8) Warnatz, J. In *Combustion Chemistry*; Gardiner, W. C., Ed.; Springer-Verlag: New York, 1984; Chapter 5.
(9) Westbrook, C. K.; Dryer, F. L. *Prog. Energy Combust. Sci.* **1984**, *10*, 1.
(10) Kerr, J. A. In *Free Radicals*; Kochi, J. K., Ed.: Wiley-Interscience: New York, 1973; Vol. 1, Chapter 1.
(11) Kerr, J. A.; Moss, S. J. *CRC Handbook of Bimolecular and Termolecular Gas Reactions*; CRC Press: Boca Raton, FL, 1981.
(12) Waage, E. V.; Rabinovitch, B. S. *Int. J. Chem. Kinet.* **1971**, *3*, 105. See also references in the following: Olson, D. B.; Gardiner, W. C. *J. Phys. Chem.* **1979**, *83*, 922.
(13) Quack, M.; Troe, J. *Ber. Bunsen-Ges. Phys. Chem.* **1974**, *78*, 240.
(14) Hase, W. L. *J. Chem. Phys.* **1976**, *64*, 2442.
(15) Wardlaw, D. M.; Marcus, R. A. *J. Phys. Chem.* **1986**, *90*, 5383.
(16) Wardlaw, D. M.; Marcus, R. A. *J. Chem. Phys.* **1985**, *83*, 3462.
(17) Troe, J. *Ber. Bunsen-Ges. Phys. Chem.* **1983**, *87*, 161.

0022-3654/88/2092-2462$01.50/0